J-7

MICROWAVE SCANNING MICROSCOPY FOR PLANAR STRUCTURE DIAGNOSTICS

Ronald J. Gutmann, Jose M. Borrego,
Prabhansu Chakrabarti, and Ming-Shan Wang

Dept. of Electrical, Computer, and Systems Engineering
Rensselaer Polytechnic Institute
Troy, New York 12180-3590

ABSTRACT

Microwave scanning microscopy is being developed to detect lateral conductivity variations in semiconductor wafers and to profile dielectric and conducting quasi-planar surfaces. We have utilized three different critically-coupled one-port cavities, with thin-diameter conducting coupling elements providing enhanced lateral sensitivity in microstrip and rectangular waveguide cavities and a circular aperture coupling element in a cylindrical waveguide cavity providing enhanced depth resolution capability. Lateral resolutions on the order of a few mils (0.002 wavelengths) and depth resolutions of a few microns (0.0001 wavelengths) have been achieved with conventional, low-power x-band instrumentation. Lateral resolution measurements of evaporated aluminum/silicon gratings with sheet conductance contrast of 300, ion-implanted n+/n silicon conductivity gratings with sheet conductance contrast of 2 and dielectrically-isolated, single-crystal-tub silicon wafers are described. More limited depth profile measurements are presented to illustrate depth resolution capability.

INTRODUCTION

Microwave scanning microscopy was originally proposed by Ash and colleagues where the ability to resolve metallic gratings, metallic images, cracks in planar metallic surfaces and dielectric discontinuities was demonstrated. Spatial resolutions as small as 0.0005λ were demonstrated using both a radiated microwave beam coupled through an aperture in a conducting plate (1-2) or a microwave signal coupled through an aperture in a ground plane in a microstrip cavity(3). These impressive resolutions were obtained using a suppressed carrier single sideband X-band signal, amplified by a 10 watt TWT, an acoustically-vibrated test station and a phase-sensitive 1 Hz bandwidth detector to obtain a 80 dB S/N ratio with a 14 mil diameter aperture.(3)

Microwave scanning microscopy is different than the more widely-developed optical scanning microscopy, where a focused optical beam is scanned relative to the specimen to improve contrast and allow electronic zoom capability(4). Optical scanning microscopy does not improve the wavelength-limited resolution of conventional optical microscopy. The optical analogy to microwave scanning microscopy is evanescent wave imagery, as developed by Lukosz(5). However, there is relatively a small activity in such ultra-resolution microscopy in the optical region because of the reduced wavelengths.

In this program we have explored the potential of microwave scanning microscopy using evanescent waves for planar structures in integrated electronics. We have achieved lateral resolution results comparable to Husain and Ash(3) with simpler microwave instrumentation, by using critically-coupled one-port cavities and have explored depth resolution capabilities as well. Results are presented illustrating the signal sensitivity to sheet conductance contrast and the feasibility of detecting features with relatively-complex dielectrically-isolated, single-crystal-tub silicon wafers. In our program emphasis has been placed on signal detection and feature recognition as a critical step in evaluating the potential of microwave scanning microscopy for integrated electronic structures.

CAVITIES UTILIZED, MEASUREMENT SET-UP AND TEST STRUCTURES

Two one-port resonant cavities were utilized for enhanced lateral resolution capability, a microstrip edge-coupled transmission line resonator with a 1 or 10 mil diameter coupling element terminating the transmission line as shown in Figure 1 and an aperture-coupled rectangular-waveguide resonator with an inductive-iris/stripline fed coupling element of similar dimensions as shown in Figure 2. In both cases the spatial extent of the dominantly-magnetic, evanescent field at the test specimen is controlled by the dimensions of the thin-conducting coupling element and the separation between the coupling element and quasi-planar test structures. Critical coupling is achieved with the microstrip cavity by adjusting the tuning disc and by adjusting the tuning screw with the rectangular waveguide cavity.

Although the lateral resolution capability with these two cavities is emphasized, a third one-port, cylindrical-waveguide resonator has been used to evaluate the potential of depth profiling. The resonator is fed at the center of the cylindrical surface and coupled to the planar test specimen through a circular aperture centered in the end surface, with critical coupling obtained with a slide-screw tuner. When operated in either

0149-645X/87/0000-0281$01.00 © 1987 IEEE

the TM_{014} or TM_{022} modes, the evanescent field in the coupling region is dominantly electric. While we were unable to laterally confine the evanescent electric field as well as the field confinement of the other two resonators, improved depth resolution was obtained.

Measurements were taken using either a circulator-coupled waveguide setup or a network analyzer in the reflection mode, with 10 mW power sources. In most cases the cavity is critically coupled without a test structure, with the quasi-planar structure resulting in an increase in reflected power and a change in resonant frequency as indicated in Figure 3. The reflected power is recorded as a function of position as the test structure is mechanically scanned, although the change in resonant frequency has been investigated for sensitivity enhancement.

Most of the test structure utilized are gratings, including evaporated aluminum gratings (0.1 μm thick) on 20 mil thick silicon wafers of nominally 10 ohm-cm resistivity and n+/n silicon gratings with ion-implanted channels forming the n+ regions. The sheet conductance contrast (i.e. ratio in the two regions) accounting for the skin depth and material thickness is 300 and 2 respectively. The effective contrast is actually higher, since the effective penetration depth of the evanescent field has not been included in the contrast calculation. Gratings were fabricated with 4 mil wide conducting regions and 35 mil spacing (4/35 gratings) and 3 mil wide conducting regions with 10 mil spacing (3/10 gratings).

In addition to these gratings, tests were performed on individual conducting lines on a variety of microwave dielectrics and, while exploring depth sensitivity, homogeneous dielectrics, semiconductors and conductors as well. Most of the results reported have focus on the lateral resolution results obtained with the grating structures with initial results on dielectrically-isolated, single-crystal-tub silicon wafers.

EXPERIMENTAL RESULTS

Mechanically scanned results with the microstrip cavity and the 4/35 silicon gratings are shown in Figures 4A and B. The data of Figure 4 was taken with a 10 mil diameter coupling element with a spacing of 4 mils between the coupling element and the quasi-planar gratings. Note that the 35 mil wide conducting regions bounding the grating have clear distinctive features and that the 4 mil wide lines in the gratings are clearly resolved, although the narrower width lines are not distinctive in the scan. The loss of feature with the reduced sheet conductance contrast of the ion-implanted n+/n silicon grating is apparent.

Similar results with the rectangular waveguide cavity are shown in Figures 5A and 5B with 1 mil diameter coupling element and a spacing of 6 mils between the coupling element and quasi-planar gratings. As with the previous results, the loss of signal sensitivity with reduced sheet conductance contrast is apparent. However,the features of the 4 mil wide highly conducting regions are more apparent with the reduced-size coupling element.

The reduction in signal amplitude with higher resolution patterns is depicted in Figure 6, which presents the results obtained with a 3/10 grating of evaporated aluminum on silicon. While the grating elements and periodicity can be resolved clearly, features such as conducting line width and sheet conductance contrast become difficult to resolve. Gratings of plated gold on alumina (sheet conductance contrast near infinity) have somewhat more distinctive features, although we have not ascertained the effect of the vertical step caused by the plating thickness.

The most ambitious test structures investigated to date are dielectrically-isolated single-crystal-tub silicon wafers, with a regular structure determined by the chip size (nominally 200 mils square). Tub dimensions vary from 5 to 53 mils with poly spacings varying from 2 to 7 mils. The wafers were processed using deep V-groove etching, oxide growth and thick CVD poly deposition, followed by etching of the original single crystal substrate. Preliminary results presented in Figure 7 demonstrate that the chip pattern and many of the tub patterns can be resolved. Clearly the conductivity contrast provided by the poly/single crystal regions is the resolution limit for our present capabilities.

Maximum depth sensitivity with different homogeneous materials was obtained with the cylindrical waveguide cavity with dominantly electric field coupling. Representative amplitude data is presented in Table 1, with the cavity critically coupled with the test materials far from the coupling element. The return loss sensitivity to depth (or spacing) varies from 0.2 dB/mil to 0.5 dB/mil depending upon the material. By measuring the resonant frequency (see Figure 3), sensitivities between 10 kHz/mil and 30 kHz/mil were determined. Since frequency changes of 1 kHz can be measured with our instrumentation, depth resolution on the order of a few microns can be obtained.

SUMMARY AND CONCLUSIONS

Microwave scanning microscopy using evanescent wave coupling from one-port critically-coupled cavities to quasi-planar test structures have demonstrated lateral resolutions on the order of a few mils (0.002λ) and depth resolution on the order of a few microns (0.0001λ) with conventional X-band instrumentation. Results on the impact of reduced conductivity contrast on resolution and signal clarity have been presented for the first time, confirming that surface layer conductivity variations are quite effective in producing detectable signals. With cavity optimization, microwave instrumentation enhancements, post-

detection signal processing, and on-test structure critical coupling, an order of magnitude improvement in these initial results are anticipated.

ACKNOWLEDGEMENT

The authors gratefully acknowledge the financial support of IBM, Essex Junction Laboratory and the supplemental equipment grants provided by New York State Science and Technology Foundation and Hewlett Packard. The support and encouragement of Dr. Henry Geipel of IBM in launching this program and the perspective of Dr. Larry Nesbit of IBM during the program are deeply appreciated. The dielectrically isolated wafers were provided by Dr. David Yaney of AT&T Bell Laboratories.

REFERENCES

1. E.A. Ash and G. Nicholls, "Super-Resolution Aperture Scanning Microscope," Nature, Vol. 237, June 1972, pp. 510-512.

2. E.A. Ash and A. Husain, "Surface Examination Using a Superresolution Scanning Microwave Microscope," Industrial Application European Microwave Conference, Sept. 1973.

3. A. Husain and E.A. Ash, "Microwave Scanning Microscopy for Non-Destructive Testing," Proceedings of the Fifth European Conference, Sept. 1975, pp. 213-217.

4. C.J.R. Sheppard, "Applications of Scanning Optical Microscopy," SPIE Vol. 368, Microscopy-Techniques and Capabilities, 1972, pp. 88-95.

5. W. Lukosz, "Imagery with Evanescent Waves," Workshop on Unconventional Imagery, Sept. 1984, pp. 73-74.

TABLE 1

RETURN LOSS DEPENDENCE UPON DEPTH
FOR HOMOGENEOUS SAMPLES
(CYLINDRICAL WAVEGUIDE CAVITY)

		Return Loss(dB)		
Depth (mils)	Conductor	Silicon 1 ohm-cm	Alumina	Silicon 300 ohm-cm
5	10.0	11.5	11.2	12.7
10	10.7	12.9	13.6	15.2
15	11.4	14.0	15.4	17.1
20	12.4	15.1	16.8	18.2
25	13.0	16.6	18.6	19.3
30	14.0	17.8	20.2	20.6
60	20.4	25.7	28.1	--

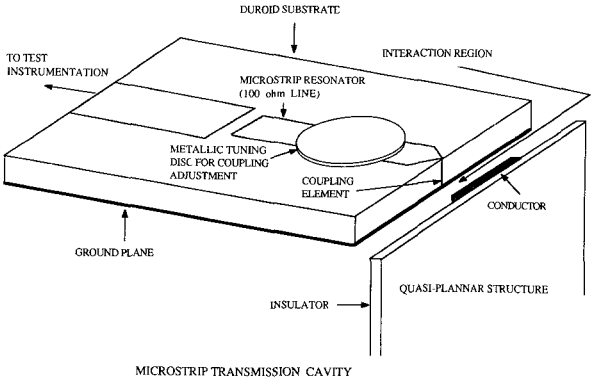

FIGURE 1

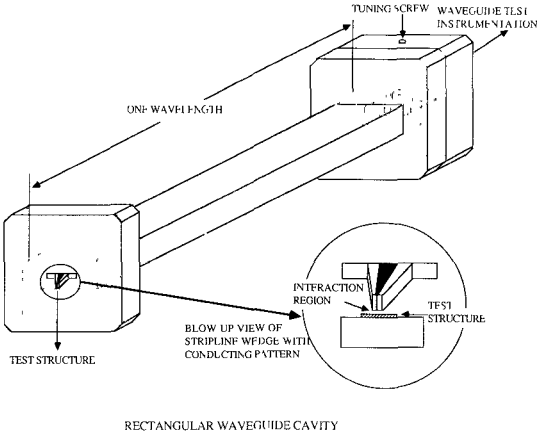

FIGURE 2

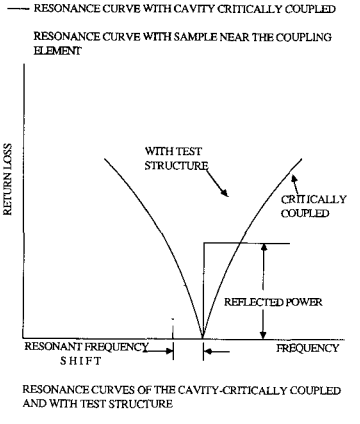

FIGURE 3

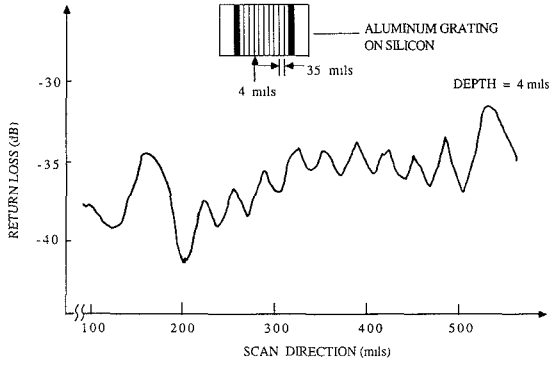

SCAN OF EVAPORATED ALUMINUM GRATING (4/35) ON SILICON WITH MICROSTRIP TRANSMISSION CAVITY (10 mil DIAMETER COUPLING ELEMENT)

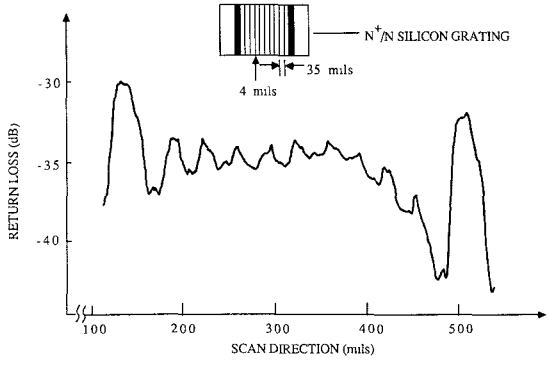

SCAN OF N^+/N SILICON GRATING 4/35 WITH MICROSTRIP TRANSMISSION CAVITY (10 mil DIAMETER COUPLING ELEMENT)

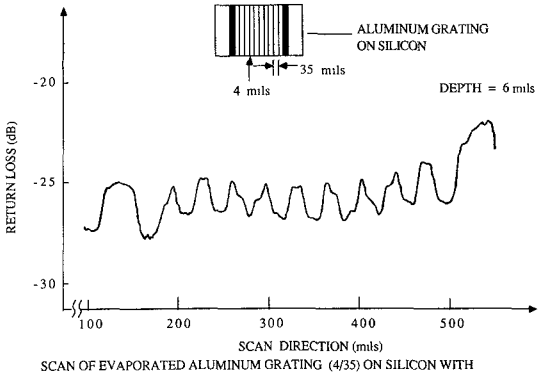

SCAN OF EVAPORATED ALUMINUM GRATING (4/35) ON SILICON WITH RECTANGULAR WAVEGUIDE CAVITY (1 mil DIAMETER COUPLING ELEMENT)

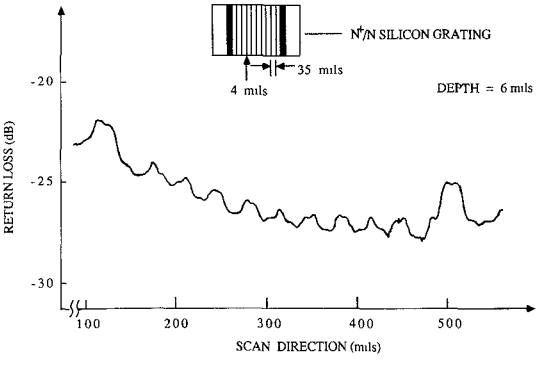

SCAN OF N^+/N SILICON GRATING 4/35 WITH RECTANGULAR WAVEGUIDE CAVITY (1 mil DIAMETER COUPLING ELEMENT)

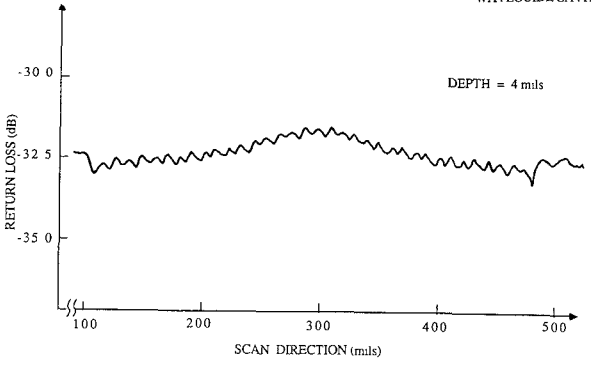

SCAN OF EVAPORATED ALUMINUM GRATING (3/10) ON SILICON WITH MICROSTRIP TRANSMISSION CAVITY (1 mil DIAMETER COUPLING ELEMENT)

FIGURE 6

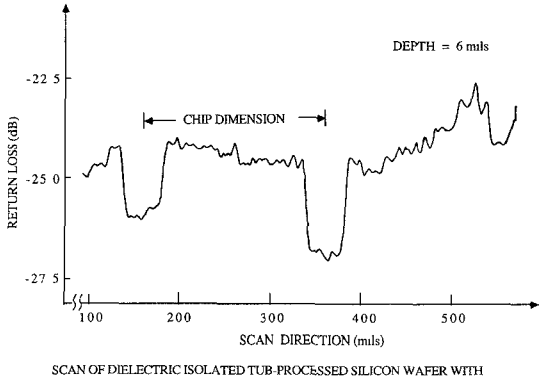

SCAN OF DIELECTRIC ISOLATED TUB-PROCESSED SILICON WAFER WITH RECTANGULAR WAVEGUIDE CAVITY (1 mil DIAMETER COUPLING ELEMENT)

FIGURE 7

A B

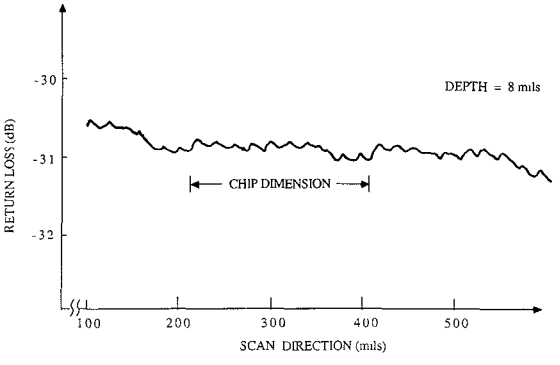

SCAN OF DIELECTRIC ISOLATED TUB-PROCESSED SILICON WAFER WITH MICROSTRIP CAVITY (1 mil DIAMETER COUPLING ELEMENT)